

DAO Office Note 1996-20

Version 1.0 Dated 2/29/2000

**Office Note Series on  
Global Modeling and Data Assimilation**

*Siegfried Schubert, Editor*

**Evaluation of RTTOV and GLA TOVS  
forward model and Jacobian**

Meta Sienkiewicz<sup>†</sup>

*Data Assimilation Office, Goddard Laboratory for Atmospheres*

*<sup>†</sup> SAIC General Sciences Corporation, Beltsville, Maryland*



Robert M. Atlas, Head  
*Data Assimilation Office*  
Goddard Space Flight Center  
Greenbelt, Maryland 20771

## Revision History

<b>Version Number</b>	<b>Version Date</b>	<b>Pages Affected/ Extent of Changes</b>	<b>Approval Authority</b>
Version 0.1	June 10, 1996	First draft (before initial review)	
Version 1	February 29, 2000	Initial release	ON Editor

**Abstract**

In this document, comparisons of the GLA and RTTOV rapid algorithms for forward radiative transfer calculations for TOVS channels are described. A description of the relevant characteristics of the forward models is given, followed by comparisons of brightness temperatures, transmittances, weighting functions and temperature Jacobians (derivative of brightness temperature with respect to input temperature). Results of timing tests for the routines are also given.

**Contents**

<b>Abstract</b>	<b>iii</b>
<b>List of Figures</b>	<b>v</b>
<b>List of Tables</b>	<b>vi</b>
<b>1 Introduction</b>	<b>1</b>
<b>2 Characteristics of the rapid algorithms</b>	<b>1</b>
<b>3 Comparison of rapid algorithm output</b>	<b>3</b>
3.1 Timing comparison . . . . .	3
3.2 Vertical discretization comparison . . . . .	6
3.3 Transmittance comparison . . . . .	6
3.4 Jacobian comparison . . . . .	8
3.5 Brightness temperature comparison . . . . .	8
<b>4 Conclusions</b>	<b>10</b>
<b>Acknowledgments</b>	<b>10</b>
<b>References</b>	<b>11</b>

**List of Figures**

1	Tropospheric GLA levels. . . . .	4
2	Tropospheric RTTOV levels. . . . .	4
3	Location of observations in the Petersen data set. . . . .	5
4	Transmittance functions for TOVS channels. . . . .	12
5	Weighting functions for TOVS channels. . . . .	15
6	Jacobians on 23 mandatory temperature levels. . . . .	18
7	Brightness temperature differences (RTTOV - GLA) for 1,750 TIGR profiles.	21
8	Brightness temperature differences (RTTOV - GLA) for Petersen profiles .	24

**List of Tables**

1	Characteristics of the rapid algorithms. . . . .	2
2	Timing tests on DAO workstations. . . . .	5
3	Comparison of calculation using input from 23 and 40 profile levels with input from the full 71 GLA levels. . . . .	7
4	Brightness temperature difference statistics (RTTOV - GLA) for 1,750 TIGR profiles. . . . .	9

## 1 Introduction

The Data Assimilation Office (DAO) is currently evaluating different methodologies for assimilation of satellite radiance observations. The prototype instrument for the evaluation of these new methodologies is the TIROS operational vertical sounder (TOVS). At the time of this study (early 1996), there were two sets of programs available to the DAO for forward calculation of TOVS radiances from atmospheric profiles; modules developed in-house using the Goddard Laboratory for Atmospheres (GLA) TOVS forward algorithm, and program modules for the RTTOV forward algorithm developed at the European Centre for Medium-range Weather Forecasts (ECMWF).

The purpose of this Office Note is to compare the GLA TOVS and RTTOV modules. This study serves two purposes. First, since the forward models were independently derived the similarity of results between the two calculations serves to validate the forward models. Second, the results of the comparison will aid in decisions regarding which algorithm to use in future work.

Please note that the results presented in this office note are not intended to determine which forward model produces more accurate results, although some deficiencies of the program suites will be mentioned.

We will start with a brief description of characteristics of the rapid algorithms (Section 2). Then comparison of results of using the rapid algorithms will be presented. The results presented include timing comparisons between calculations performed on DAO workstations (Section 3.1), comparisons of the transmittances and weighting functions (Section 3.3), Jacobians (Section 3.4) and brightness temperatures (Section 3.5) obtained using these modules.

## 2 Characteristics of the rapid algorithms

The primary characteristics of the rapid algorithms are summarized in Table 1. The GLA TOVS rapid algorithm was developed by Joel Susskind and associates at the Goddard Laboratory for Atmospheres (Susskind, *et al.* 1983) and is described in DAO Office Note 96-08 (Sienkiewicz 1996). This algorithm uses temperature, moisture and ozone input on 71 pressure levels between 1050 mb and 0.1 mb. The code was recently rewritten in modular form and modules were developed to calculate Jacobians or partial derivatives with respect to temperature, moisture, and ozone.

The RTTOV/RTATOV forward model, tangent linear model and adjoint were developed by John Eyre at ECMWF (Eyre 1991). The version evaluated here is RTTOV Version 3. The algorithm uses temperature and moisture on 40 pressure levels between 1000 mb and 0.1 mb and total column ozone as inputs. The RTATOV code extended the original RTTOV model to accommodate calculations for the next series of NOAA satellites with the AMSU microwave sounder; options were added for the use of cloud liquid water profiles and multiple microwave surface emissivity values. Further discussion of some of the entries in Table 1 follows.

**Vertical discretization** The vertical discretization (*e.g.* number and placement of pressure levels) is important for accuracy in the radiative transfer calculation; however, increased vertical resolution also leads to increased computation time. Figures 1 and 2 compare the vertical discretization of the GLA TOVS and RTTOV radiative transfer model in the troposphere to vertical levels used in the DAO's Goddard Earth Observing System (GEOS) Data Assimilation System (DAS) (DAO 1996). The left column shows some of the 20 'manda-

Characteristic	GLA	RTTOV
Pressure levels	71 levels	40 levels
Total transmittance	product of layers	sum of optical depths
Vectorized/optimized	under development	Yes
IR surface emissivity	constants for land + ocean	fixed IR emissivity ( = 1 )
MSU surface emissivity	input (retrieved)	input
Downward flux	IR - parameterized MW - Explicit integral	Explicit integral for both MW and IR
Cloud levels	none <sup>a</sup>	1 level
Solar contribution	included	not used
IR Planck function	central frequency	modified Planck
Coefficients	3 fixed gas 3 H <sub>2</sub> O, ozone	10 coefficient expansion for H <sub>2</sub> O, fixed gas
Ozone	input profile	total ozone, fixed profile
Zenith dependence	linear interpolation	explicit in coefficients

<sup>a</sup>could be implemented

Table 1: Characteristics of the rapid algorithms.

tory' pressure levels used in the analysis component of GEOS 3. In the center column, the 'levels' shown are pressure values at the sigma layer edges of the GEOS 2 atmospheric general circulation model (GCM), for a surface pressure of 1000 mb. The right column in each figure shows the vertical levels used in each forward model integration.

The spacing of integration levels for the GLA TOVS is about half that of the GEOS 2 GCM except in the boundary layer. The vertical spacing for the RTTOV forward model is somewhat variable but close to the GEOS 2 GCM spacing. The use of additional levels as in the GLA TOVS forward model should increase accuracy of the vertical integration particularly if the input profiles have a lot of detail; it also contributes to increased amount of time for the calculation. The method of calculating total transmittance also has an impact on program timing. The calculation of a sum of optical depths with subsequent exponentiation can be executed more quickly than a product of effective layer transmittances, though the impact of this would be hardware dependent. A comparison of timing for the rapid algorithms on two hardware platforms is given in Section 3.1, Table 2. Information on the effect of using coarser vertical discretization in the calculation of brightness temperature is shown in Section 3.2.

**Surface emissivity, atmospheric, solar and cloud contributions** The surface emissivity and contribution from atmospheric radiance reflected from the surface (downward flux) are handled in the same way in the two algorithms for the microwave channels. The effective downward flux is calculated explicitly through a downward integration of the radiative transfer equation. A single input value of surface emissivity is used for all microwave channels. There are provisions for additional microwave surface emissivity values to be used in AMSU calculations in RTTOV.

The two methods differ in their treatment of infrared channels, however. Kornfield and Susskind (1977) found that explicit calculation of downward IR flux (with its assumption that transmittances behave as for monochromatic calculations) gives inaccurate results. Thus, the GLATOVS model uses various parameterizations of effective IR downward flux. The code for RTTOV includes the explicit calculation, but this calculated flux is not used: since the surface emissivity is set equal to one in RTTOV, there is no contribution from

radiance reflected from the surface. In addition, though there is provision for an input solar angle there is no calculation of solar contribution in RTTOV.

There is a provision for calculation of 'partly cloudy' radiances in the RTTOV code through inclusion in the calculation of one level of opaque cloud. This is not included in the GLA retrievals but could easily be added to the GLA forward model if needed.

**Ozone** There is a significant difference in the way ozone is handled in the two forward model algorithms. The GLA forward model transmittance calculation uses input ozone profiles at 71 levels while the ozone contribution in RTTOV is a simple function of total ozone. The GLA algorithm has been used successfully to retrieve total ozone using measurements from IR channel 9 (Susskind, *et al.* 1997), while the RTTOV ozone absorption is not adequate for calculations for IR9.

In fact, the RTTOV calculation of IR9 performed in this study does not include any dependence on the vertical profiles of temperature or water vapor. The IR9 coefficients provided with the RTTOV program for the fixed gas and water vapor absorption are all zeros. Therefore, IR9 will not be included in the comparisons between GLATOVS and RTTOV transmittance functions, weighting functions, and Jacobians presented in this paper.

### 3 Comparison of rapid algorithm output

In this section, the results of some tests of the rapid algorithms are compared. The temperature, moisture, and ozone profiles used to calculate transmittances, Jacobians and brightness temperatures were from three test data sets. Two of the datasets were provided by Dr. Joanna Joiner; these were datasets that had been used in testing algorithms for the Atmospheric Infrared Sounder (AIRS). The first dataset consisted of ~80 profiles of temperature, moisture and ozone derived from an NWP model along two tracks over the southern United States (Petersen data set, see Fig. 3). The second dataset was derived from the TOVS Initial Guess Retrieval (TIGR) sounding dataset (Chedin *et al.* 1985); it contained ~1750 profiles from rawinsonde observations taken over a wide range of conditions. The third dataset, provided by Paul Piraino of the GLA Sounder Research Team, was a set of ~350 profiles generated by the TOVS Pathfinder system (Susskind *et al.* 1997). The data values in the input sets were given at the GLA rapid algorithm levels; an interpolation linear in  $\log p$  was used to obtain values at the RTTOV algorithm levels. Comparisons are made using the 4 MSU channels and 16 of the 20 HIRS channels.

The first set of results presents the timing used by each of the rapid transmittance algorithms to perform the forward model and Jacobian calculations. The second set of results shows the effect of vertical discretization on the accuracy of brightness temperatures. The third set of results compares the transmittances, Jacobians and brightness temperatures produced by the two rapid algorithms.

#### 3.1 Timing comparison

One aspect that will be important for operational use is the amount of time that it takes to calculate radiances and Jacobians. The timing for the forward model and the Jacobian calculations was tested by using the TIGR dataset of 1750 sounding profiles and performing the radiative transfer calculations 10 times per profile. Calculations were performed for only one sounding at a time, though the RTTOV/RTATOV code can be configured to calculate transmittances for multiple profiles. The timing tests were run on a Silicon Graphics 100 MHz R4000SC Indy under IRIX 5.3, with compiler options "-O -mips2". The

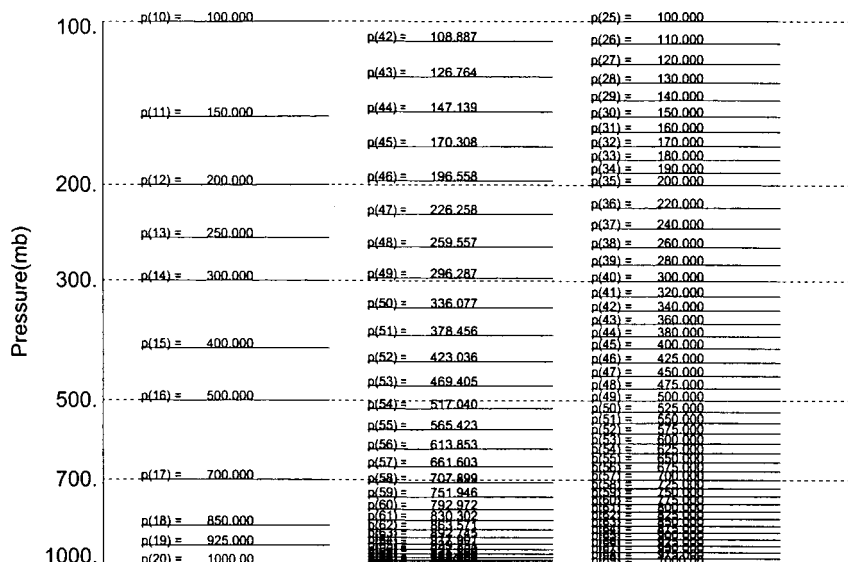


Figure 1: Tropospheric GLA levels. Left: GEOS 3 analysis levels. Center: GEOS 2 GCM sigma edges for  $p_s = 1000$ . Right: GLA TOVS forward model levels.

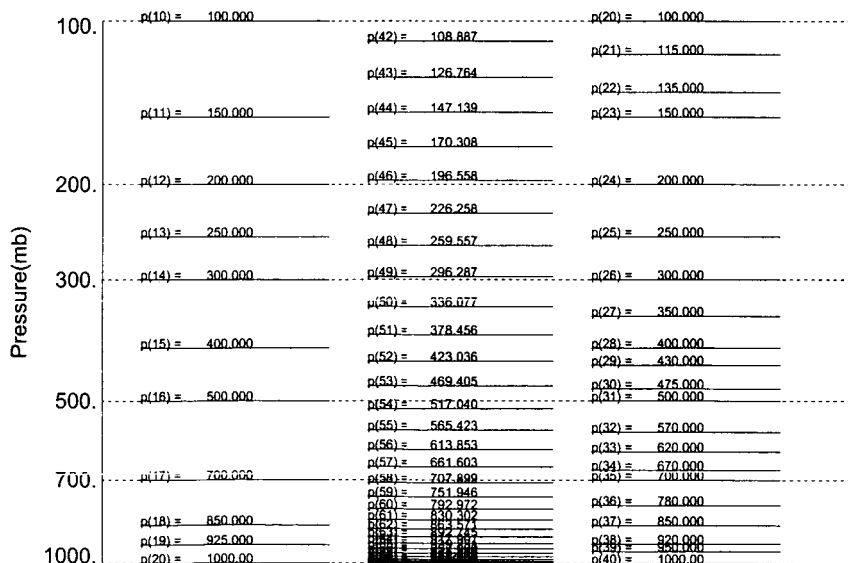


Figure 2: Tropospheric RTTOV levels. Left: GEOS 3 analysis levels. Center: GEOS 2 GCM sigma edges for  $p_s = 1000$ . Right: RTTOV forward model levels.

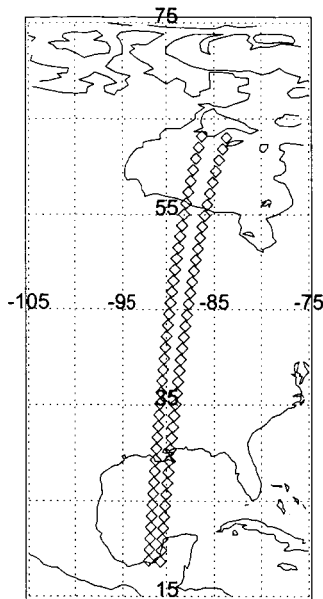


Figure 3: Location of observations in the Petersen data set.

**Timing on SGI Indy 'harrison'**

	RTTOV	GLA	GLA NO-C
Forward model	2:21	6:45	—
Jacobian	7:55	36:13	16:07

**Timing on DEC Alpha 'molotov'**

	RTTOV	GLA	GLA NO-C
Forward model	0:34	1:28	—
Jacobian	2:06	10:25	5:11

Table 2: Timing tests on DAO workstations.

calculations were performed for the 4 MSU channels and 16 of the 20 HIRS channels. For the Jacobian calculation, a simplified version of the GLA TOVS model (which omitted the effect of the mean temperature above the layer in the fixed gas derivative calculation) was also performed; this is labeled as GLA NO-C. The tests were also performed on the DAO's DEC Alpha 'molotov'. The results of the timing tests are given in Table 2.

The RTTOV/RTATOV code is much faster at performing the forward model and Jacobian calculations. The GLA code in its present configuration takes roughly 2 1/2 times as long to perform the same forward calculation as RTTOV/RTATOV and 5 times as long to perform the Jacobian calculation. These results are to be expected since the GLA model has nearly twice the vertical levels of the RTTOV/RTATOV model. The GLA TOVS model is also hampered by determining vertical transmittance through the product of layer transmittance rather than summing optical depths as in the RTTOV/RTATOV model. Additionally, the RTATOV code has been optimized to perform well on vector processing machines. While some optimization work has been performed on the GLA TOVS modules used here, the emphasis thus far has been on code readability and maintainability.

### 3.2 Vertical discretization comparison

Since the number of vertical levels used in a forward model program will influence the amount of time needed to execute the code, it is useful to examine the effect of the vertical discretization on the accuracy of the brightness temperature calculation. If fewer temperature levels are used to calculate brightness temperature, or if a lower resolution temperature profile is used as input to the forward model, we may expect the resulting brightness temperatures to be less accurate. An experiment was run using the higher resolution GLA model with lower resolution profile information to assess the effect of vertical discretization.

The input profiles used were the 350 profiles generated by the TOVS Pathfinder system (Susskind *et al.* 1997). Three sets of brightness temperatures were calculated using the GLA forward model. One set used the input profiles on the full set of GLA levels; for the other runs the profiles were first interpolated to a coarser resolution and then interpolated back to the full 71 levels to simulate the effect of lower vertical resolution. The interpolations performed were linear interpolations with respect to the logarithm of pressure. The coarser grids used were (a) a set of 23 mandatory pressure levels (similar to the analysis levels pictured in Fig. 1) and (b) the 40 RTTOV levels. The statistics for differences between the calculation with 71 input levels and the other calculations are given in Table 3.

The brightness temperatures calculated using the coarsest resolution (23 mandatory levels) input differed substantially from the brightness temperatures calculated using the original profiles. The standard deviations of brightness temperature differences were all greater than 0.1K. The largest difference in mean brightness temperature was in channel IR 9, where the difference was more than 1 degree. The IR9 results may have been influenced by the decreased resolution of ozone and water vapor inputs as well as temperatures.

When the input profiles were provided on the 40 RTTOV pressure levels, the agreement between the calculated brightness temperatures and the brightness temperatures calculated from the original profiles was much better. There was still a significant bias in IR 1 and IR 9, but not as much as for the coarser profiles. The standard deviations were also much less for most of the channels. All the standard deviations were less than 0.2K and most were less than 0.1K. One interpretation of these results is that use of input for vertical discretization coarser than the 40 RTTOV levels could lead to significant inaccuracies in the output brightness temperatures.

### 3.3 Transmittance comparison

Figure 4 shows transmittance functions from GLA TOVS and RTTOV for 19 of the TOVS channels. The curves shown are the average transmittance for 1750 profiles from the TIGR dataset, calculated at nadir, with a surface pressure of 1000 mb. The transmittances were quite similar for most of the channels although a few appeared to be displaced slightly in the vertical between the two methods. The largest discrepancies were for the channels IR1, MW4, and IR4 which are sensitive to upper atmospheric conditions.

Figure 5 shows the weighting functions  $\partial\tau/\partial\ln p$  generated from the two algorithms. As with the transmittances, the weighting functions are average values for 1750 profiles from the TIGR test data set. The weighting functions are similar, except for IR1 which has a broader peak for the GLA calculations. These weighting functions are generally smooth though there are a few anomalous features in some of the channels for one or the other of the methods. For example, the RTTOV weighting function for IR12 has an unusual peak at 100 mb. In the RTTOV forward model the atmospheric absorption for the portion of the spectrum observed by IR12 is zero above 100 mb, and then increases to a value near to that modeled by the GLATOVS, hence causing the peak in the weighting function. This is probably an error in the RTTOV coefficients. The similarity between the results of the two forward models in general is quite encouraging since, as noted in the introduction, it helps

**(a) Results for input on 23 mandatory pressure levels**

Channel	Mean Tb	Mean difference	Std. deviation
MW1	241.896	-0.0269662	0.303507
MW2	244.635	-0.0791696	0.193703
MW3	222.408	-0.0342313	0.103521
MW4	210.657	-0.00171895	0.137516
IR1	233.960	0.789136	0.297411
IR2	217.605	0.134709	0.113834
IR4	226.966	0.000766083	0.149176
IR5	239.412	0.0525839	0.211170
IR6	249.694	0.0347208	0.251028
IR7	260.637	0.0254096	0.264104
IR8	277.649	0.0247850	0.259373
IR9	254.911	1.21655	0.513883
IR10	273.769	-0.0260738	0.247598
IR11	251.688	-0.109435	0.428532
IR12	233.568	-0.208948	0.479979
IR13	265.354	-0.0939787	0.261813
IR14	255.963	-0.0998166	0.270032
IR15	245.087	-0.0298170	0.208362
IR18	277.243	-0.0423452	0.116627
IR19	277.700	-0.0322018	0.116173

**(b) Results for input on 40 RTTOV pressure levels**

Channel	Mean Tb	Mean difference	Std. deviation
MW1	241.896	0.00514187	0.0624652
MW2	244.635	0.00247047	0.0400525
MW3	222.408	0.0328029	0.0791486
MW4	210.657	0.0792184	0.178393
IR1	233.960	-0.236700	0.113818
IR2	217.605	-0.00211047	0.121434
IR4	226.966	-0.0104757	0.0563021
IR5	239.412	-0.0175604	0.0498292
IR6	249.694	-0.00634309	0.0495419
IR7	260.637	-0.0106788	0.0530934
IR8	277.649	-0.00344400	0.0492524
IR9	254.911	0.270187	0.0808105
IR10	273.769	-0.00795025	0.0479693
IR11	251.688	0.0172831	0.0841593
IR12	233.568	0.0457260	0.128555
IR13	265.354	-0.0294197	0.0573253
IR14	255.963	-0.0366359	0.0657564
IR15	245.087	-0.0702011	0.0845403
IR18	277.243	-0.00826712	0.0224495
IR19	277.700	-0.00746408	0.0227313

Table 3: Comparison of calculation using input from 23 and 40 profile levels with input from the full 71 GLA levels.

to validate the differing forward models.

### 3.4 Jacobian comparison

The comparison of Jacobians for the two rapid algorithms is not as straightforward as comparison of transmittances. The Jacobian is defined as the derivative of the brightness temperature with respect to input values of the rapid algorithm. We would expect these to differ since the input temperature and moisture profiles are given at different levels. For our purposes, the most relevant comparison for the Jacobians is not with respect to the input parameters of the rapid algorithms, but with respect to the model or analysis variables from which the input values are derived. By specifying a set of input temperature, moisture and ozone levels and a transformation from that input set to the 40 or 71 vertical levels of the rapid algorithms, we can assess the response of the modules to the same set of inputs.

For this comparison, it is assumed that input values are on only 23 mandatory pressure levels, and that interpolation that is linear with  $\log p$  is used to obtain the profiles for the rapid algorithms. In that case we can write temperature on a rapid algorithm level  $T_i$  as a linear combination of the input temperatures  $\tilde{T}_j$ :

$$T_i = \sum_{j=1}^M a_{ij} \tilde{T}_j \quad (1)$$

Then, the temperature Jacobian for the mandatory pressure level  $k$  can be written as:

$$\frac{\partial \theta}{\partial \tilde{T}_k} = \sum_{i=1}^N \frac{\partial \theta}{\partial T_i} \frac{\partial T_i}{\partial \tilde{T}_k} = \sum_{i=1}^N a_{ik} \frac{\partial \theta}{\partial T_i} \quad (2)$$

Thus, the effect of the transformation from the input levels to the rapid algorithm levels can be applied by multiplying the rapid algorithm Jacobians by the interpolation weighting matrix  $a_{ik}$ .

The 23-level temperature Jacobians for the GLA and RTTOV algorithms are shown in Fig. 6. As with the transmittance figures, the curves plotted are the average curves for the 1750 TIGR soundings used in the comparison. The curves appear somewhat irregular because they have not been normalized (*i.e.* the values were not divided by  $\delta \ln p$  for appropriate pressure layers). As with the transmittance functions, the largest differences between the algorithms is for channel IR1. Channels IR4-7 also show differences near 100 mb. The results from the two algorithms are again quite similar overall.

### 3.5 Brightness temperature comparison

The last set of comparisons to examine is the comparison of brightness temperatures obtained from the two rapid algorithms. Fig. 7 shows scatter plots of brightness temperature differences between temperatures calculated using RTTOV and those calculated using the GLA modules, using the TIGR profiles as input. Difference statistics are shown in Table 4. We see there are substantial systematic differences between the brightness temperatures for some of the channels. The largest differences were for channel IR9—the RTTOV calculation is nearly useless for this channel since ozone absorption is not included. Other channels (IR1, IR8, IR15, IR18, and IR19) had mean differences of 2.0 – 2.6 K. The mean difference in IR1 can be attributed to the variation in the location of the weighting function peak for that channel which was noted earlier. The IR15 difference is also from differences in weighting functions; from Figs. 5 and 6 we note that the weighting function is slightly

Channel	Mean Tb	Mean difference	Std. deviation
MW1	263.413	0.0576781	0.0553120
MW2	242.362	-0.163909	0.0671784
MW3	223.714	-0.0108094	0.0812112
MW4	215.342	-0.268382	0.812425
IR1	235.942	-2.01163	0.990777
IR2	222.060	0.277693	0.191740
IR4	227.761	-0.277896	0.480513
IR5	237.980	-0.247820	0.363921
IR6	246.104	-0.0999504	0.331212
IR7	254.560	1.61980	0.420399
IR8	266.225	2.29353	0.498169
IR9	250.124	19.0127	6.91581
IR10	263.635	1.51216	1.03445
IR11	250.899	0.231715	0.955204
IR12	236.936	1.49609	1.26222
IR13	256.772	-1.93561	0.485202
IR14	249.468	-0.599558	0.203396
IR15	241.042	-2.54579	0.737519
IR18	265.372	2.59240	0.577293
IR19	265.843	2.59128	0.416265

Table 4: Brightness temperature difference statistics (RTTOV - GLA) for 1,750 TIGR profiles.

higher for RTTOV, hence the positive bias. Channels IR8, IR18, and IR19 are window channels and so these differences probably result from differences between the surface emissivity parameters used in the two methods. Most notably, the RTTOV surface contribution would not include any atmospheric influence since the emissivity is set to 1 (see Table 1).

The standard deviations of differences between brightness temperatures are also substantial, and in some cases exceed the expected noise level of the TOVS instrument. However, these standard deviations may not be representative of actual atmospheric conditions. The distribution of soundings in the TIGR dataset does not match that of the real atmosphere. The TIGR dataset includes proportionately more of the outlying and unusual sounding conditions than a random sampling of the real atmosphere would contain (Chedin *et al.* 1985). Thus we may expect these estimates of standard deviation to be larger than what would be found in the real atmosphere.

Some of the plots in Fig. 7 show one particular outlier point with a rather large brightness temperature difference; the profile associated with that point was quite warm through the troposphere but had a very cold tropopause around 100 mb. From Fig. 6 we see that the RTTOV algorithm gives more weight at 100 mb than the GLA algorithm; this accounts for the discrepancy in brightness temperatures for that point. This is a good example of the state dependence of the differences between the brightness temperatures. For this particular sounding, we also know that either one or both of the forward models is producing brightness temperatures that are quite inaccurate. Thus, this illustrates another characteristic of the forward models, that they are more accurate for profiles similar to those used to fit the transmittance model coefficients and will give worse results for less typical atmospheric conditions.

Fig. 8 shows differences for brightness temperatures calculated using the Petersen data set (see Fig. 3 for locations). These differences agree in general with those from the TIGR

data set. The plots appear to show a systematic relation of the differences with respect to brightness temperature. This is an artifact of the choice of profiles in the Petersen dataset; the temperature and moisture profiles vary rather smoothly along the 'track' and so state-dependent differences in brightness temperature also change smoothly. The results do hold some promise for application of bias corrections to the derived radiances. Bias corrections could be calculated near locations where other information (e.g. co-located rawinsonde data) is available. However, this example also shows one must be careful not to overfit based on a small sample of data.

## 4 Conclusions

We have compared the GLA TOVS and RTTOV forward radiance model routines for TOVS. Each set of routines has some advantages. The GLA TOVS program handles ozone (especially IR channel 9) better. The RTTOV program executes faster and has some framework for later inclusion of ATOVS channels.

Both sets of routines produce comparable transmittance functions, weighting functions, and Jacobians, though there are some notable differences in a few of the channels. The brightness temperatures produced by these programs may differ considerably, with some channels showing a substantial mean difference in calculated brightness temperatures. These mean differences have been related to differences in transmittance coefficients and surface emissivity calculation. The standard deviation of the differences between calculated brightness temperatures was also substantial, though this could have resulted from the variance in the sounding profile datasets used. The forward models are most accurate for typical atmospheric profiles. For unusual profiles the difference in calculated brightness temperatures between the two methods may be substantial, hence one or both methods would be inaccurate.

**New Developments (October 1999)** Development of rapid forward models has continued since the writing of this Office Note. Concerns about errors in the RTTOV model in water vapor channels prompted development of the OPTRAN model (McMillan *et al.* 1995 a,b). Improvements have also been made to the RTTOV model – among other things ozone profiles are now used as input (rather than total column ozone), resulting in improved simulation of IR9 which is sensitive to ozone (Rizzi and Matricardi 1998, Saunders *et al.* 1999). The Sounder Research Team under Joel Susskind plans to use a newer rapid algorithm based on the AIRS model developed by Larrabee Strow for further HIRS research (Susskind 1999, personal communication). The Data Assimilation Office will have more choice about the rapid algorithm to be used in conjunction with their next assimilation system.

In many respects the results of this paper have been superseded. The methods for comparison presented here will be useful in evaluation of the newer rapid algorithms as they become available. This study can serve as a baseline for future studies in rapid transmittance algorithms at the DAO.

## Acknowledgments

Joanna Joiner and Paul Piraino supplied the test data sets used in this study. Dr. Joiner was also instrumental in obtaining the RTTOV program for use by the DAO. The excellent reviews by Laurie Rokke and Steve Cohn resulted in substantial improvements to this paper.

## References

- Chedin, A., N.A. Scott, C. Wahiche, and P. Moulinier, 1985: The improved initialization inversion method: A high resolution physical method for temperature retrievals from the satellites of the *TIROS-N* series. *J. Climate Appl. Meteor.*, **24**, 128-143.
- DAO, 1996: *Algorithm Theoretical Basis Document Version 1.01*, Data Assimilation Office, NASA Goddard Space Flight Center, Greenbelt, MD 20771. Available online from <http://dao.gsfc.nasa.gov/subpages/atbd.html>.
- Eyre, J.R., 1992: A fast radiative transfer model for satellite sounding systems. *ECMWF Technical Memorandum No. 176*.
- Kornfield, J., and J. Susskind, 1977: On the effect of surface emissivity on temperature retrievals. *Mon. Wea. Rev.*, **105**, 1605-1608.
- McMillan, L.M., L.J. Crone, M.D. Goldberg, and T.J. Kleespies, 1995a: Atmospheric transmittance of an absorbing gas. 4. OPTRAN: a computationally fast and accurate transmittance model for absorbing gases with fixed and with variable mixing ratios at variable viewing angles. *Appl. Opt.*, **34**, 6269-6274.
- McMillan, L.M., L.J. Crone, and T.J. Kleespies, 1995b: Atmospheric transmittance of an absorbing gas. 5. Improvements to the OPTRAN approach. *Appl. Opt.*, **34**, 8396-8399.
- Rizzi, R. and M. Matricardi, 1998: The use of TOVS clear radiances for numerical weather prediction using an updated forward model. *Quart. J. Roy. Meteor. Soc.*, **124**, 1293-1312.
- Saunders, R., M. Matricardi, and P. Brunel, 1999: An improved fast radiative transfer model for assimilation of satellite radiance observations. *Quart. J. Roy. Meteor. Soc.*, **125**, 1407-1425.
- Sienkiewicz, M., 1996: The GLA TOVS rapid algorithm Forward radiance modules and Jacobian Version 1.0. *DAO Office Note 96-08*, Data Assimilation Office, NASA Goddard Space Flight Center, Greenbelt, MD 20771.
- Susskind, J., and J.E. Searl, 1977: Synthetic atmospheric transmittance spectra near 15 and 4.3  $\mu\text{m}$ . *J. Quant. Spectrosc. Radiat. Transfer*, **19**, 195-215.
- Susskind, J., J. Rosenfield, and D. Reuter, 1983: An accurate radiative transfer model for use in the direct physical inversion of HIRS2 and MSU temperature sounding data. *J. Geophys. Res.*, **88**, 8550-8568.
- Susskind, J., J. Rosenfield, and D. Reuter, 1984: Remote sensing of weather and climate parameters from HIRS2/MSU on TIROS-N. *J. Geophys. Res.*, **89**, 4677-4697.
- Susskind, J., P. Piraino, L. Rokke, L. Iredell, and A. Mehta, 1997: Characteristics of the TOVS Pathfinder Path A Dataset. *Bull. Amer. Meteor. Soc.*, **78**, 1449-1472.

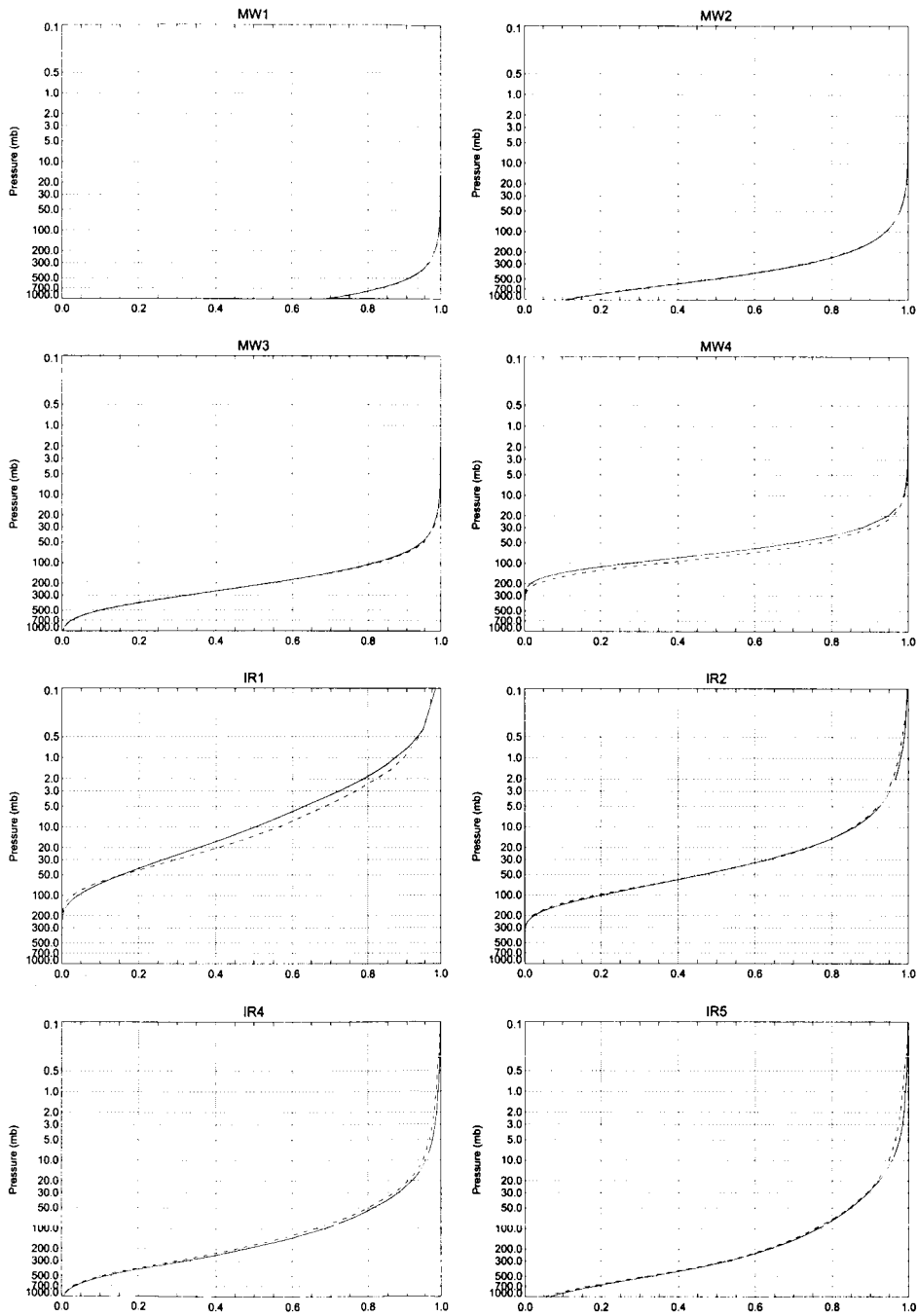


Figure 4: Transmittance functions for TOVS channels. Solid line: GLA rapid algorithm. Dashed line: RTTOV.

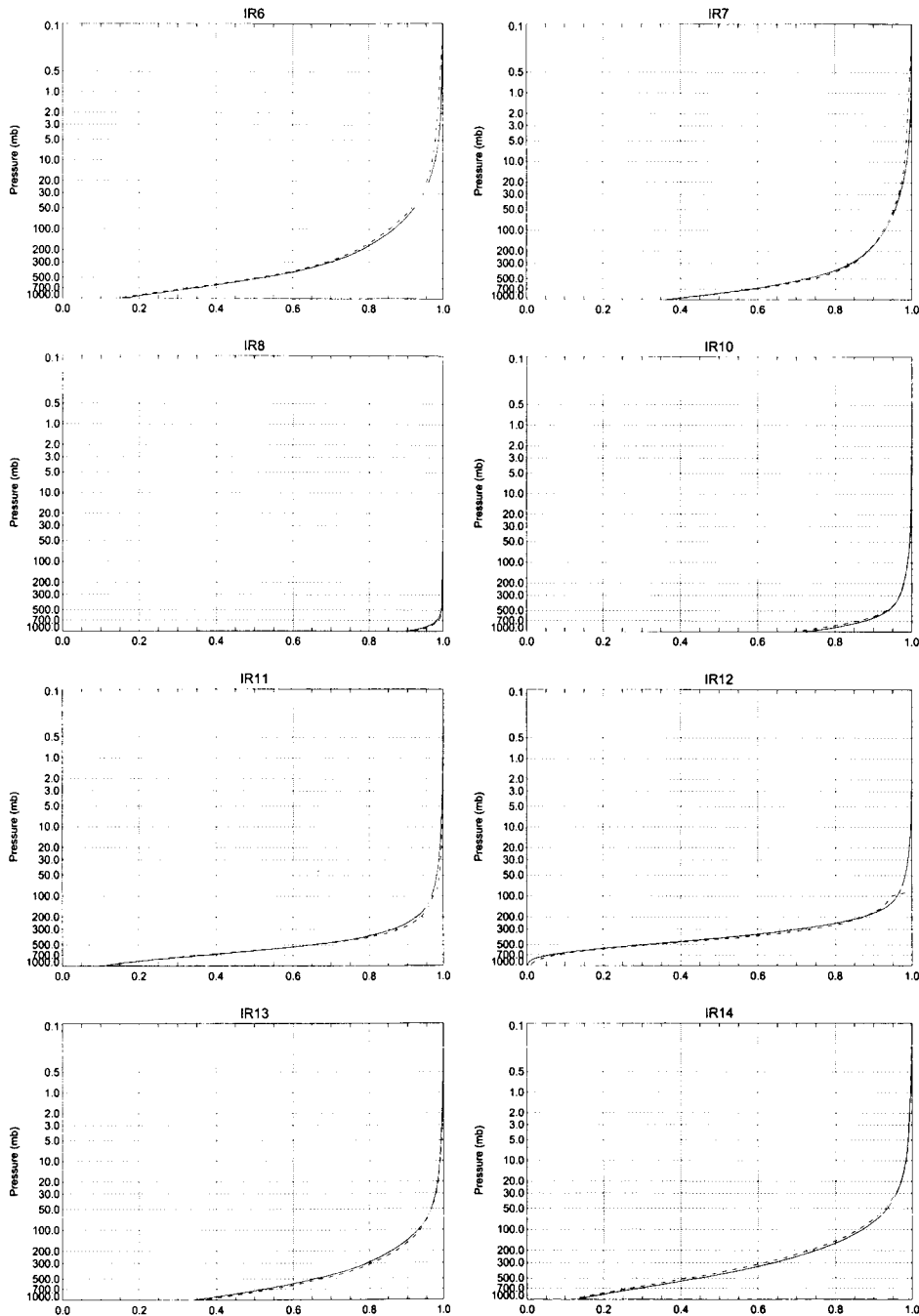


Figure 4 (continued): Transmittance functions for TOVS channels. Solid line: GLA rapid algorithm. Dashed line: RTTOV.

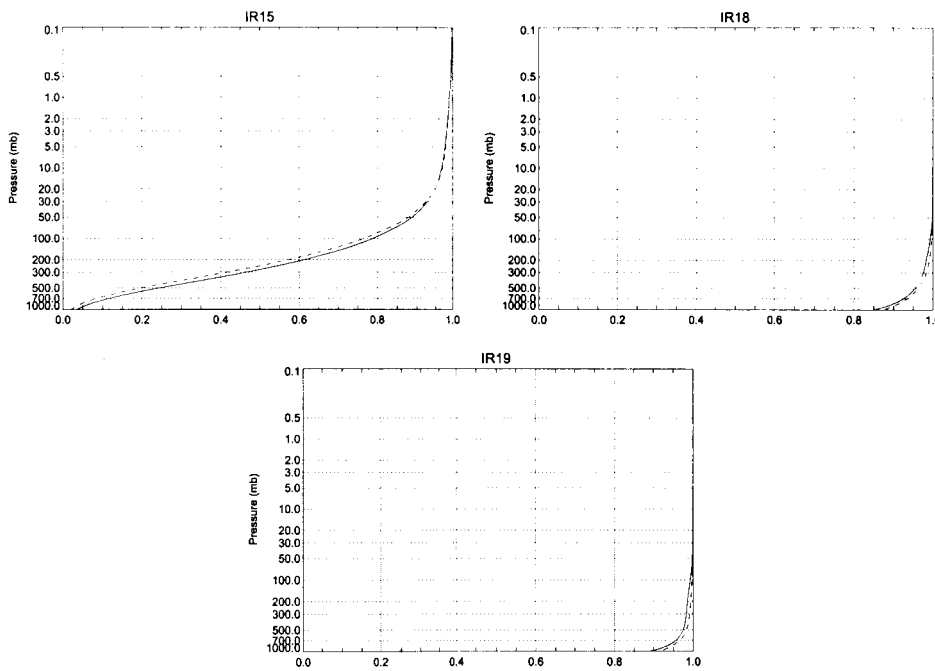


Figure 4 (continued): Transmittance functions for TOVS channels. Solid line: GLA rapid algorithm. Dashed line: RTTOV.

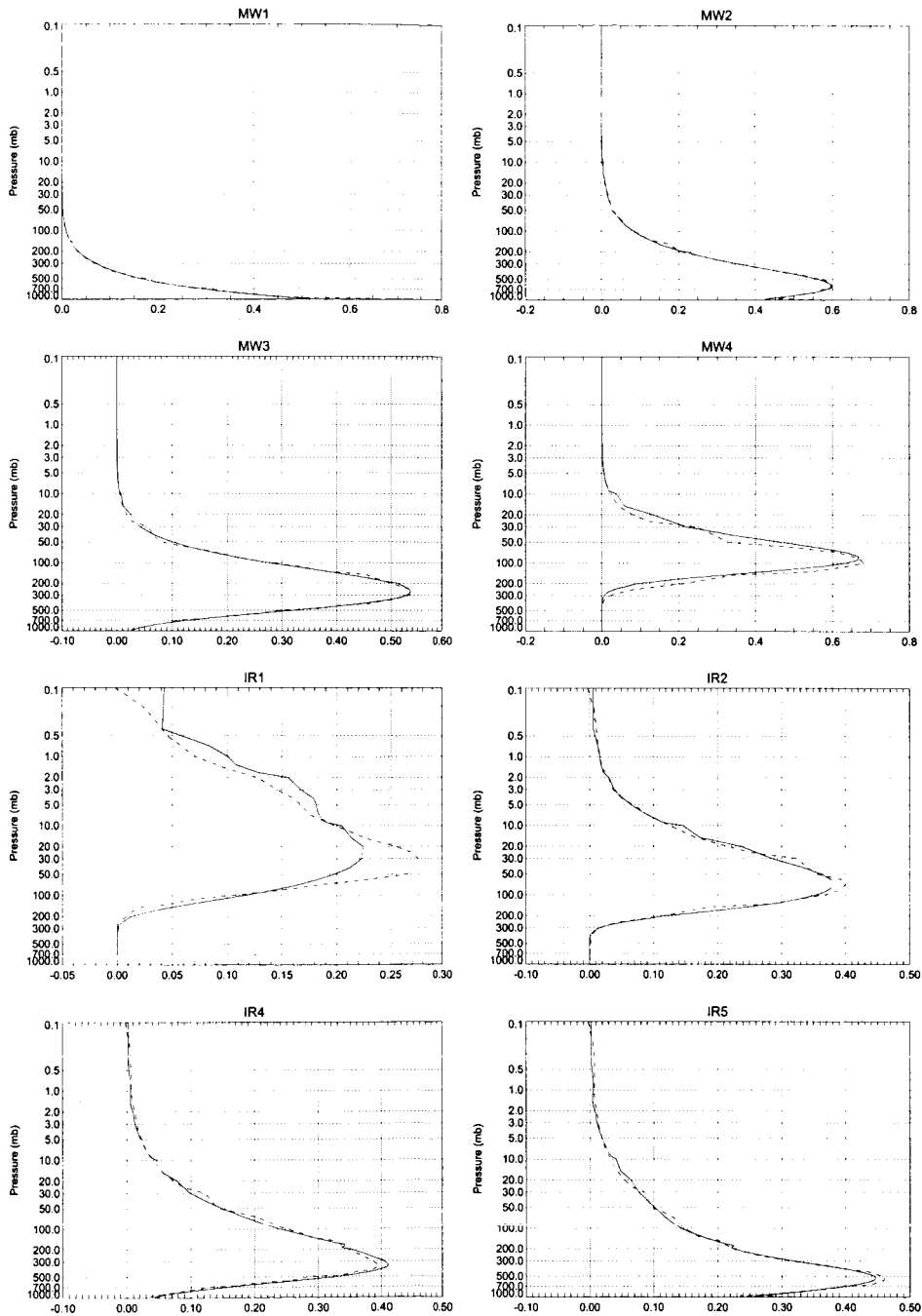


Figure 5: Weighting functions  $\partial\tau/\partial\ln p$  for TOVS channels. Solid line: GLA rapid algorithm. Dashed line: RTTOV.

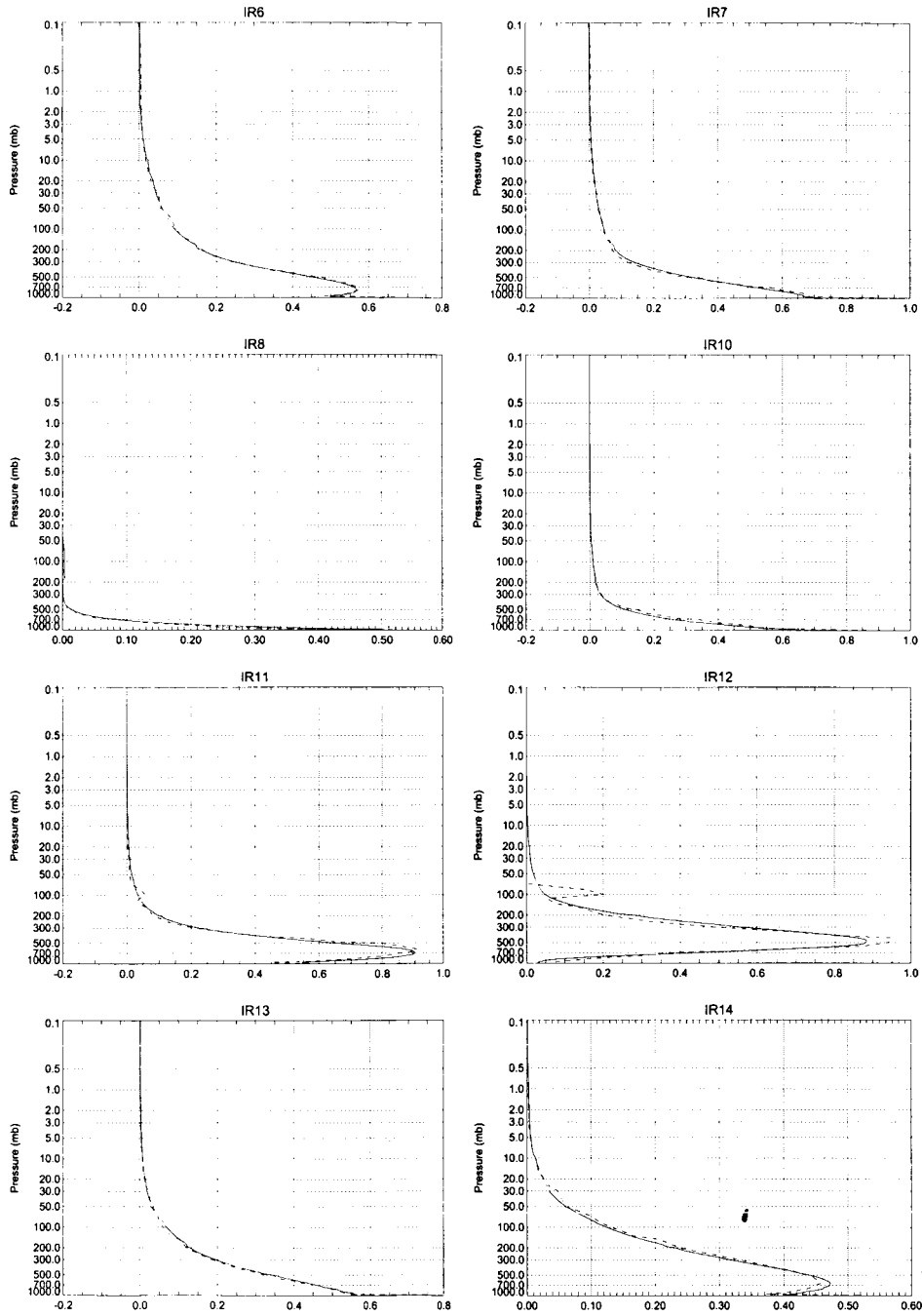


Figure 5 (continued): Weighting functions  $\partial\tau/\partial\ln p$  for TOVS channels. Solid line: GLA rapid algorithm. Dashed line: RTTOV.

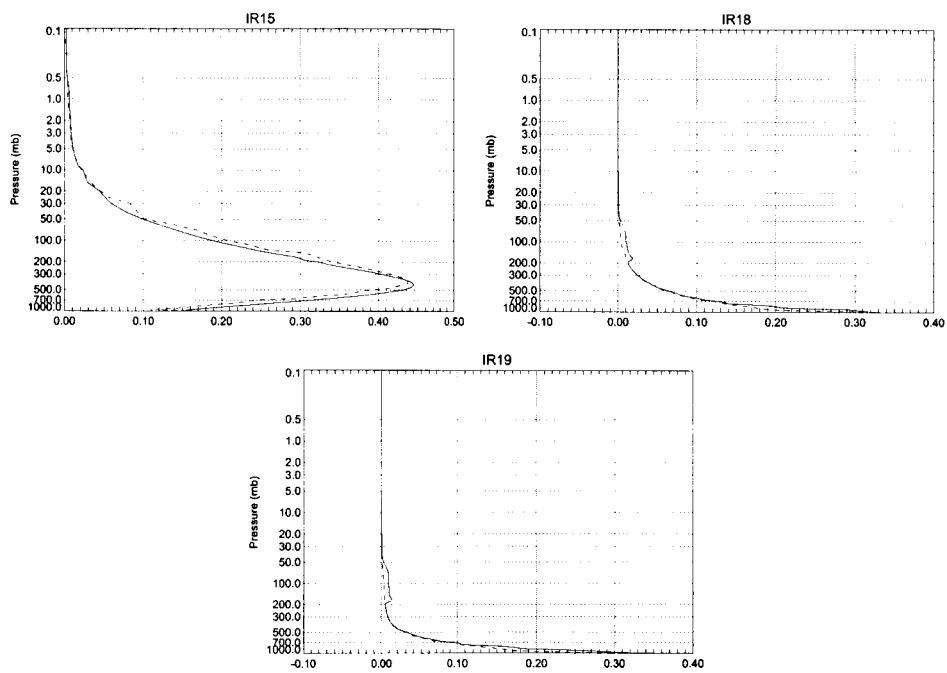


Figure 5 (continued): Weighting functions  $\partial\tau/\partial\ln p$  for TOVS channels. Solid line: GLA rapid algorithm. Dashed line: RTTOV.

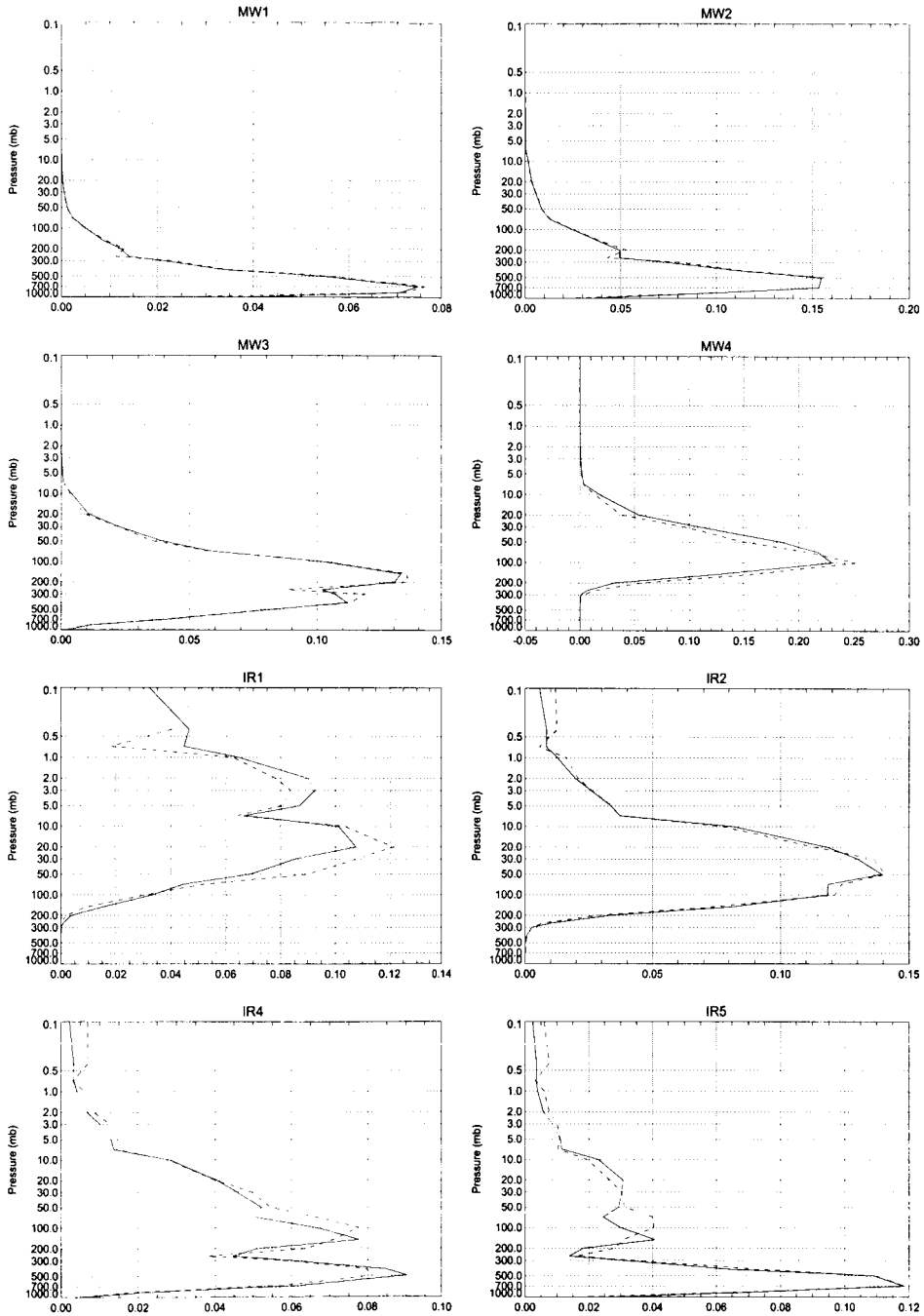


Figure 6: Jacobians for input temperatures on 23 mandatory temperature levels. Solid line: GLA rapid algorithm. Dashed line: RTTOV.

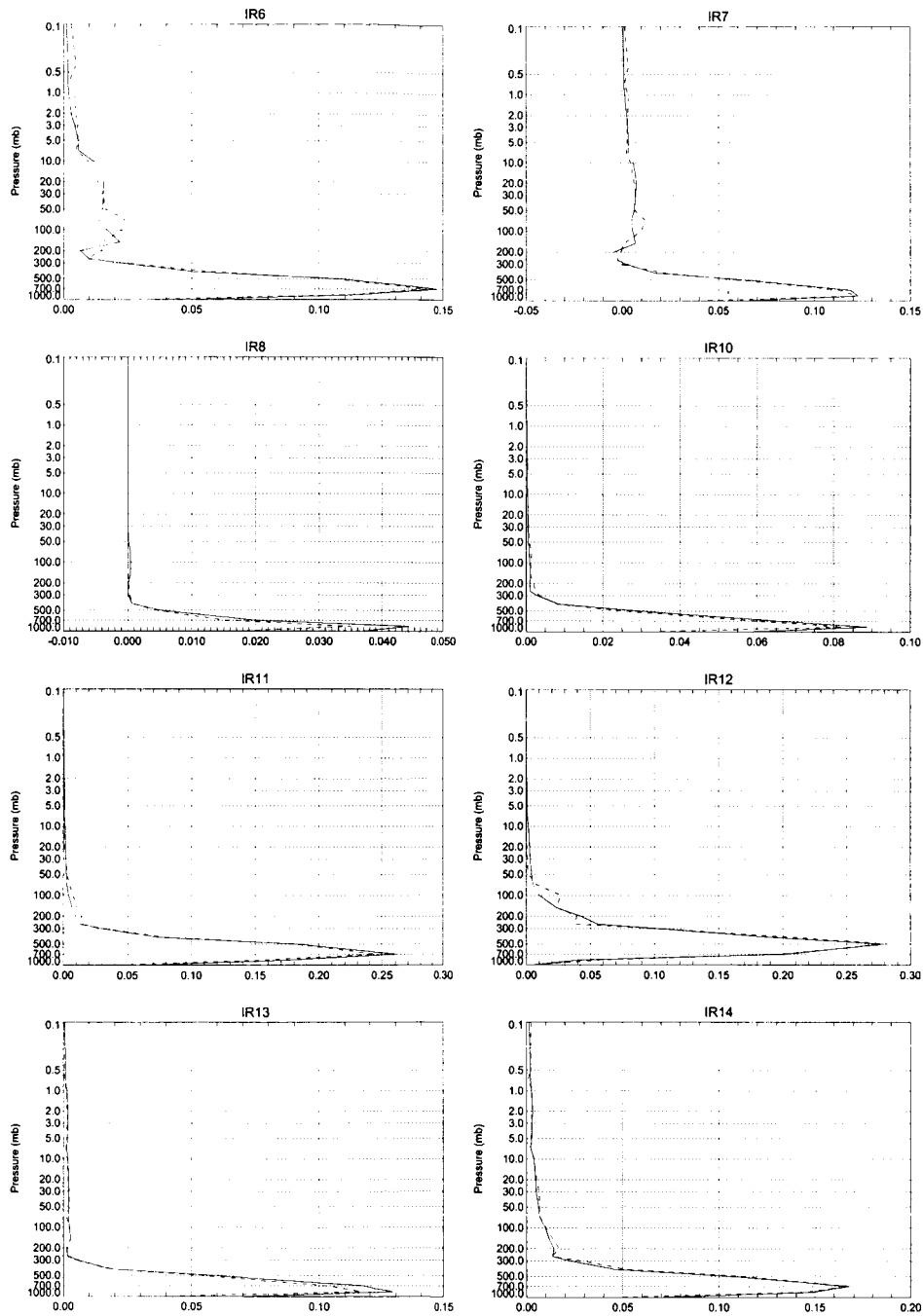


Figure 6 (continued): Jacobians for input temperatures on 23 mandatory temperature levels. Solid line: GLA rapid algorithm. Dashed line: RTTOV.

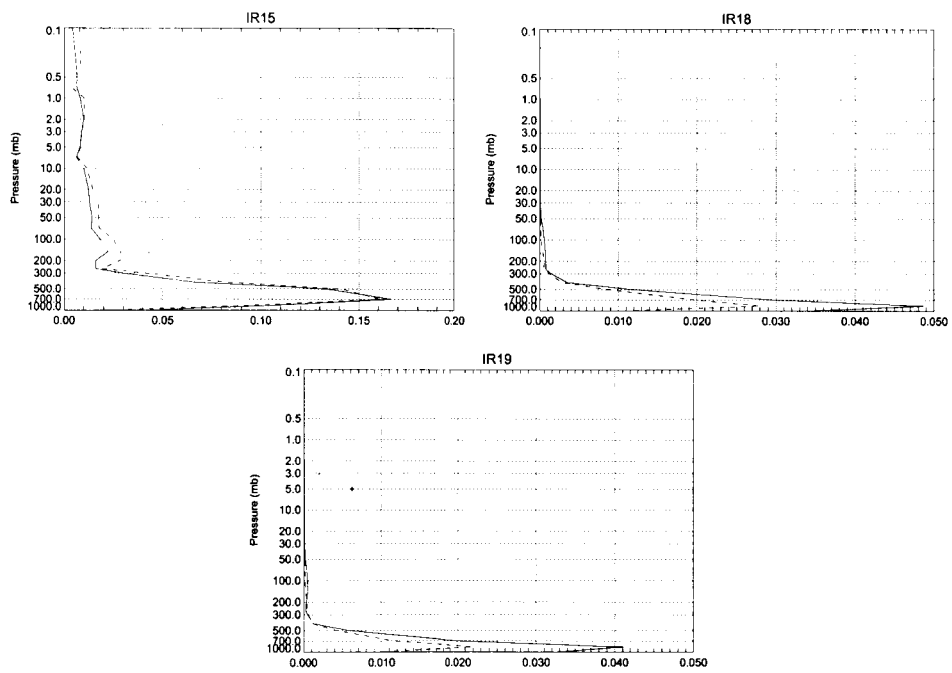


Figure 6 (continued): Jacobians for input temperatures on 23 mandatory temperature levels. Solid line: GLA rapid algorithm. Dashed line: RTTOV.

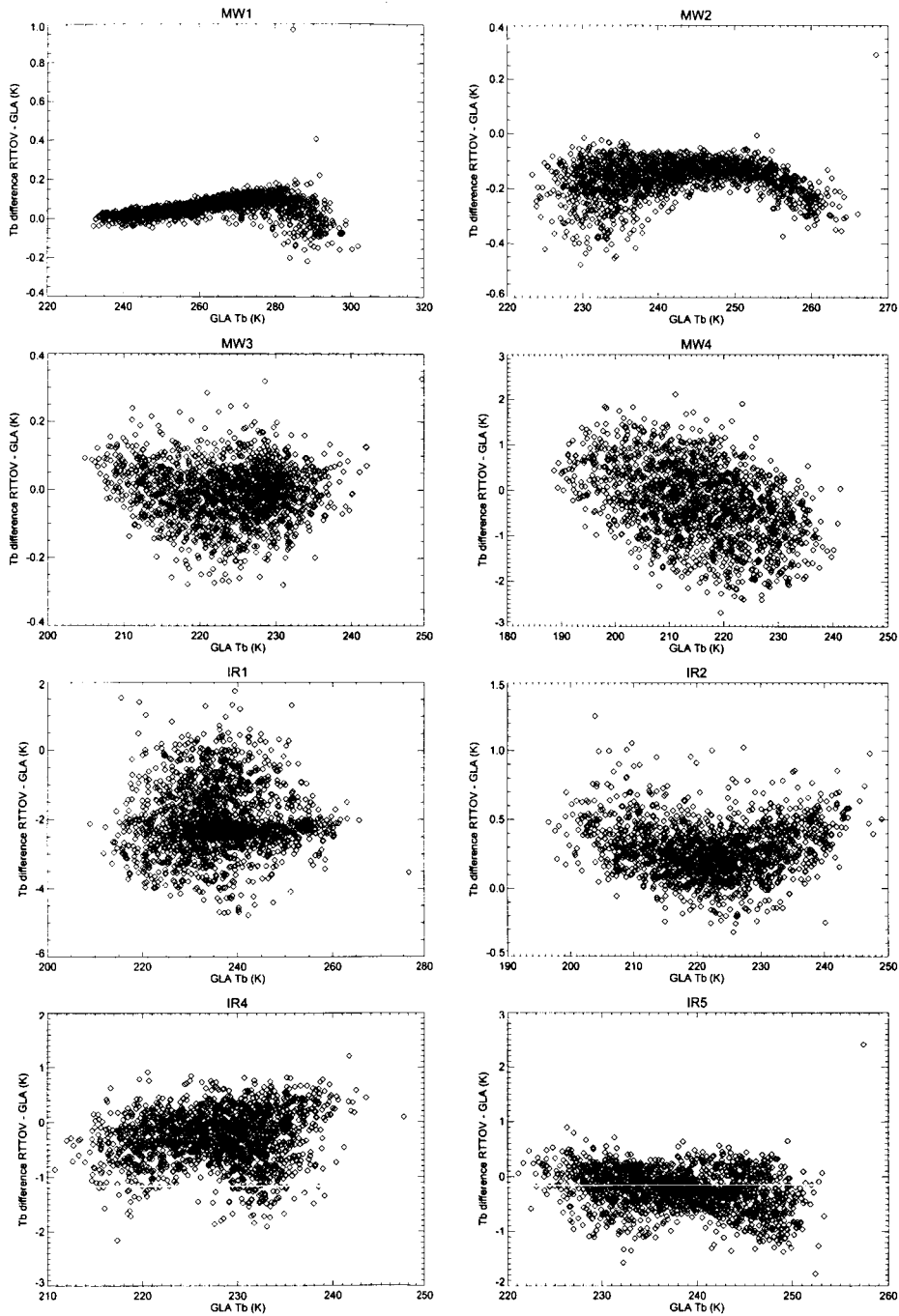


Figure 7: Brightness temperature differences (RTTOV - GLA) for 1,750 TIGR profiles.

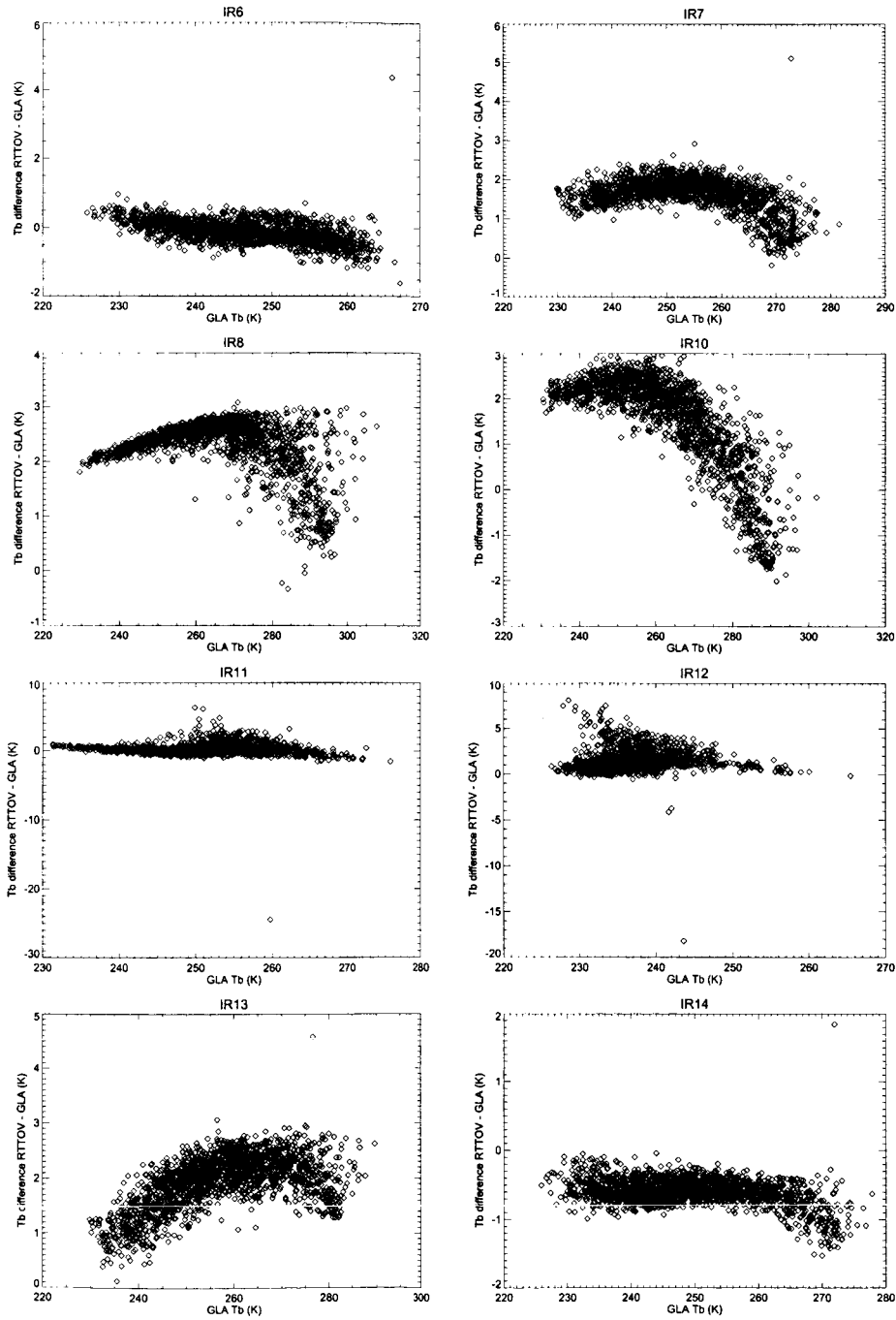


Figure 7 (continued): Brightness temperature differences (RTTOV - GLA) for 1,750 TIGR profiles.

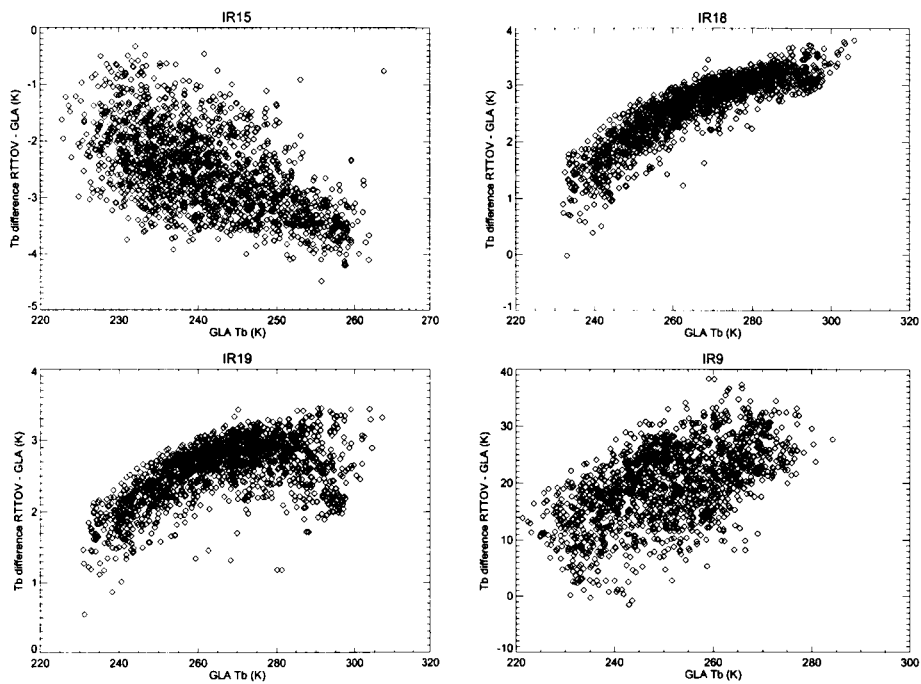


Figure 7 (continued): Brightness temperature differences (RTTOV - GLA) for 1,750 TIGR profiles.

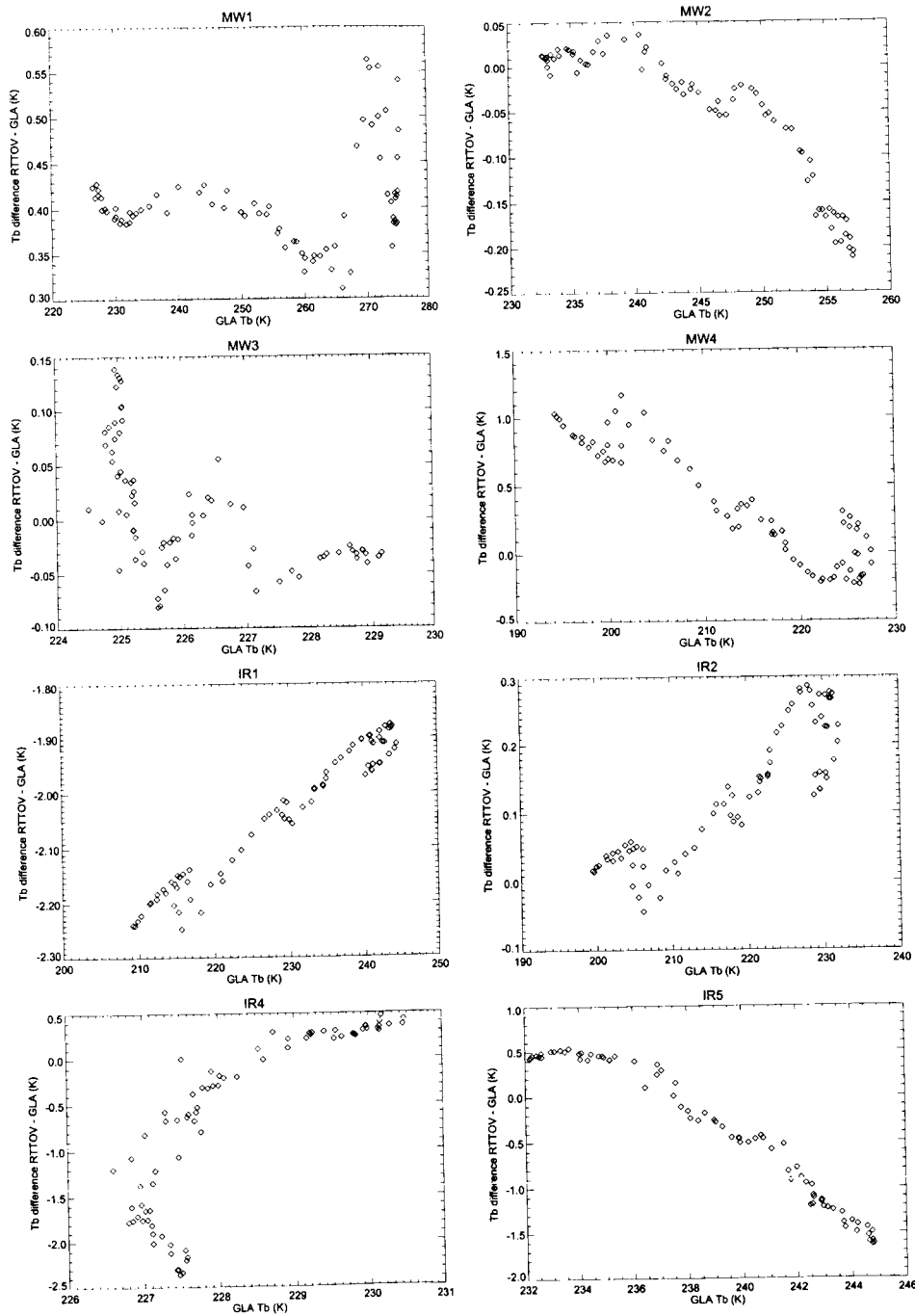


Figure 8: Brightness temperature differences (RTTOV - GLA) for Petersen profiles

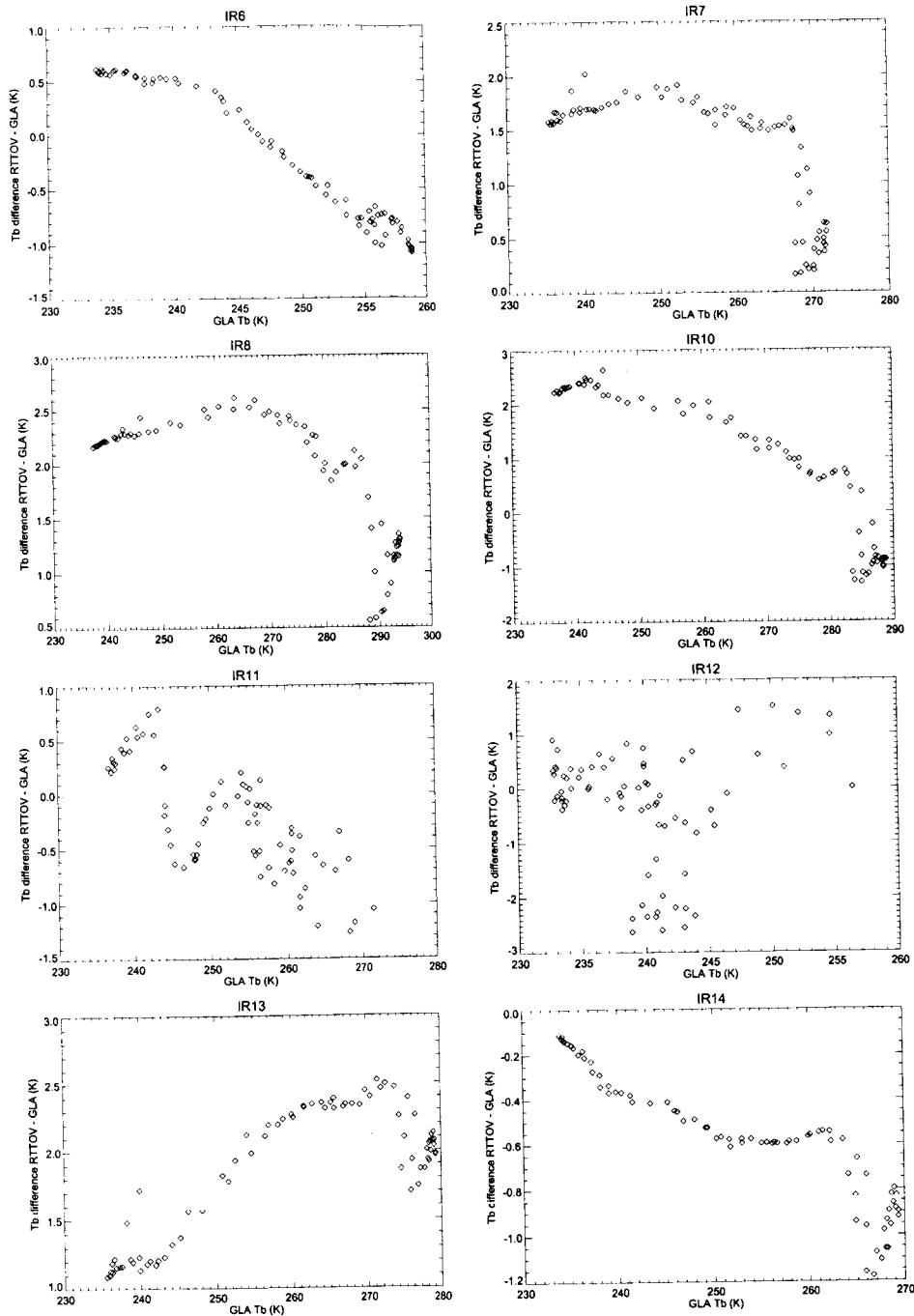


Figure 8 (continued): Brightness temperature differences (RTTOV - GLA) for Petersen profiles.

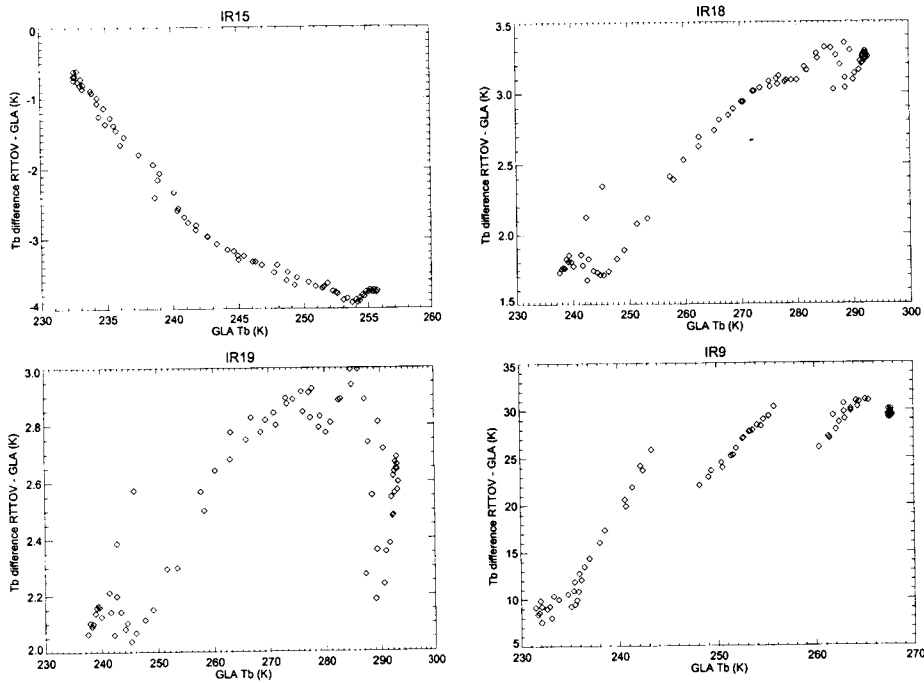


Figure 8 (continued): Brightness temperature differences (RTTOV - GLA) for Petersen profiles.